

NONDESTRUCTIVE ANALYSIS OF TEXTURES IN ROLLED SHEETS BY ULTRASONIC TECHNIQUES

M. SPIES and E. SCHNEIDER

Fraunhofer-Institut für zerstörungsfreie Prüfverfahren, Saarbrücken, FRG

(Received February 8, 1988, in final form December 7, 1989)

The preferred grain orientation in polycrystals causes a direction dependence of the ultrasonic wave velocities. In an extensive study, the texture influence on different ultrasonic wave velocities is measured in series of cold-rolled ferritic steel sheets. Based on that, ultrasonic techniques are developed to characterize the texture in terms of the three fourth-order expansion coefficients of the orientation distribution function (ODF). Evaluation equations are given for the application of free ultrasonic longitudinal and shear waves as well as for the application of ultrasonic SH-waves.

Furthermore, linear correlations are found between the Δr - and r_m -values, characterizing the deep drawability of the sheets and the expansion coefficients C_4^{13} and C_4^{11} , evaluated by ultrasonic techniques. The study demonstrates that ultrasonic techniques hold high promise to evaluate the fourth-order expansion coefficients of the ODF and to characterize the deep drawing behavior of rolled sheets by the use of calibration experiments.

KEY WORDS Elastic anisotropy, ultrasonic wave velocity, pulse-echo-overlap, texture coefficients, plastic anisotropy.

1. INTRODUCTION

Textures in rolled sheets are developed during production by deformation processes and heat treatments. Thus magnetic, elastic and plastic properties of the product become direction dependent. This can be desirable, but it can also have negative effects. In both cases a nondestructive analysis of the texture and its consequences for material behavior is of great interest. X-ray diffraction is the mostly known method of texture determination. A variation of this method is industrially used for some years. Ultrasonic techniques provide additional information, they allow texture analysis in the surface as well as in the bulk of rolled sheets. Both X-ray and ultrasonic techniques evaluate the anisotropy caused by texture and provide a nondestructive determination of the deep drawing behavior of rolled sheets on the basis of theoretical and empirical relations between texture and plastic deformation.

2. THEORY

2.1 Orientation Distribution Function

Texture is the orientation distribution of the single crystals in the polycrystalline aggregate.

Texture is mathematically described by the orientation distribution function (ODF). This function displays the probability to find a single crystal in the polycrystalline sample with a certain orientation with respect to the sample coordinate system. After Bunge (1965) the ODF can be written as a series expansion into symmetrical generalized spherical harmonics:

$$f(g) = \sum_{l=0}^{\infty} \sum_{\mu=1}^{M(l)} \sum_{\nu=1}^{N(l)} C_l^{\mu\nu} \dot{T}_l^{\mu\nu}(g), \quad (1)$$

where g : orientation, $\dot{T}_l^{\mu\nu}$: symmetrical generalized spherical harmonics, $C_l^{\mu\nu}$: expansion coefficients.

The upper limits $M(l)$ and $N(l)$ depend on l and on the crystal and sample symmetry, respectively. The $\dot{T}_l^{\mu\nu}(g)$ form an orthonormal function system; they are invariant towards all rotations of the sample symmetry (indicated by the right dot) and towards all rotations of the crystal symmetry (indicated by the left two dots). For further details see e.g. Bunge (1982).

A similar representation of the ODF was given by Roe (1965), a comparison between his terminology and the one by Bunge was given by Esling, Bechler-Ferry and Bunge (1982).

2.2 Ultrasonic Velocities in Cubic Materials with Rolling Texture

During the rolling of cubic materials (steels, aluminium-alloys) an orthorhombic texture is developed, which is characterized by three orthogonal mirror planes. Because of the cubic crystal symmetry on the one hand, and the orthorhombic sample symmetry on the other, only the three fourth-order expansion coefficients C_4^{11} , C_4^{12} and C_4^{13} need to be considered for texture description in first approximation (Pursej and Cox, 1954, Bunge, 1968). Inserting the elastic constants for the textured polycrystal in Voigt-approximation (Bunge, 1968) into Christoffel's Equation (see e.g. Auld 1973), the following propagation velocities for free ultrasonic waves (shear and longitudinal) in cubic materials with rolling texture result:

$$\begin{aligned} \rho v_{11}^2 &= c_{11} - c \left(\frac{2}{5} - \frac{1}{70} \sqrt{\frac{7}{3}} \left(C_4^{11} - \frac{2}{3} \sqrt{5} C_4^{12} + \frac{1}{3} \sqrt{35} C_4^{13} \right) \right) \\ \rho v_{22}^2 &= c_{11} - c \left(\frac{2}{5} - \frac{1}{70} \sqrt{\frac{7}{3}} \left(C_4^{11} + \frac{2}{3} \sqrt{5} C_4^{12} + \frac{1}{3} \sqrt{35} C_4^{13} \right) \right) \\ \rho v_{33}^2 &= c_{11} - c \left(\frac{2}{5} - \frac{1}{70} \sqrt{\frac{7}{3}} \frac{8}{3} C_4^{11} \right) \\ \rho v_{12}^2 &= c_{44} + c \left(\frac{1}{5} + \frac{1}{70} \sqrt{\frac{7}{3}} \left(\frac{1}{3} C_4^{11} - \frac{1}{3} \sqrt{35} C_4^{13} \right) \right) = \rho v_{21}^2 \\ \rho v_{23}^2 &= c_{44} + c \left(\frac{1}{5} - \frac{1}{70} \sqrt{\frac{7}{3}} \left(\frac{4}{3} C_4^{11} + \frac{2}{3} \sqrt{5} C_4^{12} \right) \right) = \rho v_{32}^2 \\ \rho v_{31}^2 &= c_{44} + c \left(\frac{1}{5} - \frac{1}{70} \sqrt{\frac{7}{3}} \left(\frac{4}{3} C_4^{11} - \frac{2}{3} \sqrt{5} C_4^{12} \right) \right) = \rho v_{13}^2 \end{aligned} \quad (2)$$

where $c = c_{11} - c_{12} - 2c_{44}$.

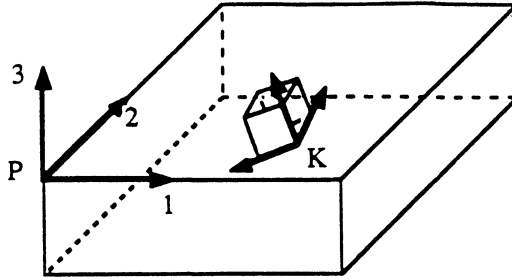


Figure 1 Sample fixed coordinate system P and crystal fixed system K for characterization of orientation. ($1 \hat{=}$ rolling direction, $2 \hat{=}$ transverse direction, $3 \hat{=}$ normal direction).

The first subscript of the velocity v indicates the propagation direction, the second one indicates the polarization direction of the wave. 1, 2 and 3 represent the rolling, transverse and normal direction according to Figure 1. ρ is the density and c_{ij} are the single-crystal elastic constants.

Out of the numerous possibilities to determine the expansion coefficients $C_4^{1\nu}$ from Eqs. (2) Spies (1989) selected those which best fit the requirement of low error propagation. With λ and μ being the Lamé constants, the resulting equations appear as follows:

$$C_4^{11} = \frac{210}{8c} \sqrt{\frac{3}{7}} \left(2\mu - (c_{11} + 2c_{44}) \frac{V_{31}^2 + V_{32}^2}{V_{31}^2 + V_{32}^2 + V_{33}^2} \right) \quad (3)$$

$$C_4^{12} = \frac{210}{4\sqrt{5}c} \sqrt{\frac{3}{7}} \left((c_{11} + 2c_{44}) \frac{V_{31}^2 - V_{32}^2}{V_{31}^2 + V_{32}^2 + V_{33}^2} \right) \quad (4)$$

$$C_4^{13} = \frac{210}{8\sqrt{35}c} \cdot \sqrt{\frac{3}{7}} \left(6\mu - \lambda + (c_{11} + 2c_{44}) \frac{V_{33}^2 + 8 \cdot V_{12}^2}{V_{31}^2 + V_{32}^2 + V_{33}^2} \right) \quad (5)$$

The velocity of ultrasonic waves propagating in the plane of a rolled plate, i.e. guided modes of the plate are given by Thompson, Smith and Lee (1985). Considering the effect of the so called beam skewing, Sayers and Proudfoot (1986) derive the following equation for the velocity of the SH_0 -mode:

$$\begin{aligned} \rho v_{SH_0}^2(\theta) = & \mu + \frac{1}{70} \sqrt{\frac{7}{3}} c \left(\frac{1}{3} C_4^{11} - \frac{1}{3} \sqrt{35} C_4^{13} + \frac{8}{3} \sqrt{35} C_4^{13} \cos^2 \theta \sin^2 \theta \right. \\ & \left. \times \left(1 - \frac{1}{70} \sqrt{\frac{7}{3}} \frac{16}{3} \sqrt{35} \frac{c}{\mu} C_4^{13} \cdot (1 - 2 \cos^2 \theta)^2 \right) \right). \end{aligned} \quad (6)$$

Here θ is the angle between rolling direction and propagation direction, ρ is the density, μ is the shear modulus and again $c = c_{11} - c_{12} - 2c_{44}$. Beam skewing is due to the fact that in highly anisotropic media the group velocity vector does not coincide with the phase velocity vector. This is the case for the SH-wave measurements performed in this work (see 3. Experimental), where the phase velocity of waves is measured whose group velocity vector lies along the direction given by θ . Equation (6) accounts for this effect, which vanishes at the angles

$\theta = 0^\circ, 45^\circ$ and 90° . Solving Eq. (6) for C_4^{11} provides

$$C_4^{11} = \frac{210}{2c} \sqrt{\frac{3}{7}} \{ \rho (V_{SH_0}^2(0^\circ) + V_{SH_0}^2(45^\circ)) - 2\mu \}. \quad (7)$$

Further manipulation of the equation resulting for C_4^{13} leads to (Spies, 1989)

$$C_4^{13} = \frac{210\mu}{32\sqrt{35}c} \sqrt{\frac{3}{7}} \cdot (1 - 2 \cos^2 \theta)^{-1} \cdot \left(1 - \sqrt{1 - 16 \frac{(1 - 2 \cos^2 \theta)^2}{\cos^2 \theta \sin^2 \theta} \frac{V_{SH_0}(\theta) - V_{SH_0}(0^\circ)}{V_{SH_0}(0^\circ)}} \right). \quad (8)$$

By measuring the velocities of different ultrasonic wave modes, Eqs. (3) to (5), (7) and (8) allow the determination of the texture-characterizing expansion coefficients C_4^{1v} .

2.3 Plastic Anisotropy

Of technological or industrial importance is not the texture by itself, but its consequence, the plastic anisotropy, which determines the deep drawability of rolled sheets. For characterization of the deep drawing properties the Lankford-parameter, also called r -value, is widely used (Lankford, Snyder, Bauscher, 1950). This value is determined in a tensile test where the changes of thickness d and width b of a strip is measured after a plastic deformation of at least 20%. The r -value is then determined according to the relationship

$$r = \frac{\ln(b_0/b_\epsilon)}{\ln(d_0/d_\epsilon)}, \quad (9)$$

where 0 designates the initial, ϵ the final state.

The quantity q is defined by

$$q = \frac{r}{r+1} \quad (10)$$

and has also found widespread application. The values

$$r_m = \frac{1}{4} [r(0^\circ) + 2r(45^\circ) + r(90^\circ)] \quad (11)$$

and $\Delta_r = \frac{1}{2} [r(0^\circ) - 2r(45^\circ) + r(90^\circ)]$

are used to evaluate the deep drawability and the effect of earing, respectively (Vlad, 1972). They are determined in a tensile test with strips cut at $0^\circ, 45^\circ$ and 90° to the rolling direction.

The linear correlations between the fourth-order expansion coefficients and the plastic anisotropy parameters r_m and Δ_r result from the empirical relationships between the r -values and Young's modulus on the one hand and the theoretical relationship between Young's modulus and the expansion coefficients C_4^{1v} on the other hand.

With E_m and ΔE defined as

$$E_m = \frac{1}{4} [E(0^\circ) + 2E(45^\circ) + E(90^\circ)]$$

and $\Delta E = \frac{1}{2} [E(0^\circ) - 2E(45^\circ) + E(90^\circ)], \quad (12)$

Stickels and Mould (1970) confirmed linear correlations between E_m and r_m and ΔE and Δr , respectively, on a large number of low-carbon steel sheets.

The theoretical relationship between the $C_4^{1\nu}$ and Young's modulus E is described by Bunge (1968, 1982). This relationship states that Young's modulus E measured in a certain direction to the rolling direction, which is described by the angle θ , can be written as

$$E(\theta) = E_r + E_1 C_4^{11} + E_2 C_4^{12} \cos 2\theta + E_3 C_4^{13} \cos 4\theta \quad (13)$$

Thereby E_r is the average mean value of Young's modulus, and E_1 , E_2 and E_3 are constants containing the single crystal elastic constants.

From this a linear correlation between C_4^{11} and r_m on the one hand and C_4^{13} and Δr on the other hand is expected. Thus, by determining the expansion coefficients of the fourth order, ultrasonic techniques give the possibility to determine parameters which characterize the plastic anisotropy of rolled sheets.

Earlier Bunge (1970) dealt with the relation between the expansion coefficients $C_1^{\mu\nu}$ and q in a theoretical work. However, a determination of q taking into consideration only the fourth-order expansion coefficients was reported to be too rough (Bunge, 1982b). But it corresponds to the approximation underlying the Stickels and Mould relationship.

3. EXPERIMENTAL

The expansion coefficients $C_4^{1\nu}$ can be determined by measuring the ultrasonic velocity of different wave modes according to Eqns. (3) to (5), (7) and (8). The ultrasonic velocity measurements are performed using the pulse-echo-overlap method, which is described in detail by Papadakis (1967). The ultrasonic set-up to be used for measurements with shear and longitudinal waves consists of an ultrasound apparatus (MATEC) which generates pulses of approximately $1 \mu\text{s}$ duration and of variable repetition rate. These pulses are impressed on commercial transducers which are acoustically bonded to the specimen. The reflected r.f. echoes are received by the same transducers, amplified and displayed on the screen of an oscillo-scope. Two of the displayed echoes are then chosen to determine the time-of-flight. Commercial two-channel oscilloscopes allow—with the help of a constant time reference—time-of-flight measurements with an accuracy of $\pm 1 \text{ ns}$.

The measurements with SH-waves are performed using electromagnetic-ultrasonic transducers (EMATs). A transmitter and a receiver—built with their characteristics to fit the sheets under test (wavelength $\lambda = 4 \text{ mm}$, frequency $f \sim 800 \text{ kHz}$)—were screwed to a bar and thus held at a fixed distance of $S = 100 \text{ mm}$. This arrangement can be set onto the sheets at different angles between the rolling direction of the sheets and the propagation direction of the SH-waves. The system used mainly consists of a pulse generator which synchronizes the gate for the transmitting pulse and the trigger of an oscilloscope. The acoustic pulse echoes from the specimen are transformed into electrical voltage pulses by the receiver-EMAT, demodulated in a superposition receiver and shown on the screen of the oscillo-scope, the time-of-flight measurement being performed in the same way as described above.

In all cases the parameter measured is the time-of-flight as a function of the orientation of the polarization and propagation direction, respectively, towards the rolling direction of the sheets. The times-of-flight are measured manually according to the pulse-echo-overlap method; an automatic device for the measurement of time-of-flight is now also available. The pathlengths are the sample thicknesses or the transmitter-receiver distances. Particularities of the experimental set-ups and the performed measurements are given elsewhere (Spies, 1989).

4. RESULTS

Different series (series I and II) of cold-rolled ferritic steel sheets were tested, with the r_m - and Δr -values provided by the manufacturer. For series II corresponding samples from the center (c) and the edge (e) of the coil were available. Additionally one series (series 0), for which the expansion coefficients of the ODF had been determined, was available.

To show the efficiency of the applied ultrasonic techniques, the fourth-order expansion coefficients C_4^{1v} were determined using Eqs. (3), (4) and (8), and compared to the C_4^{1v} determined by X-ray diffraction (reflection method). This is shown in Figure 2a) to c). If it is considered that the X-ray values bear an error of up to $\pm 10\%$ and that the difference in the depth of penetration for both techniques is several orders of magnitude, the results are quite satisfactory. However, for one sample the C_4^{1v} -ultrasonic value does not compare at all with the X-ray value, and is therefore left out in Figure 2a).

The aim of this work is not a direct comparison of X-ray and ultrasonic techniques, but the assessment of the deep drawability of steel sheets with ultrasonics.

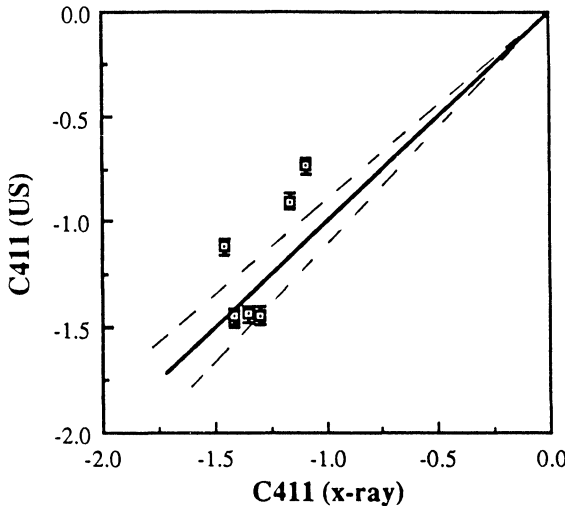


Figure 2(a). Correlation between the expansion coefficient C_4^{11} determined by ultrasonics and by X-ray diffraction for series 0.

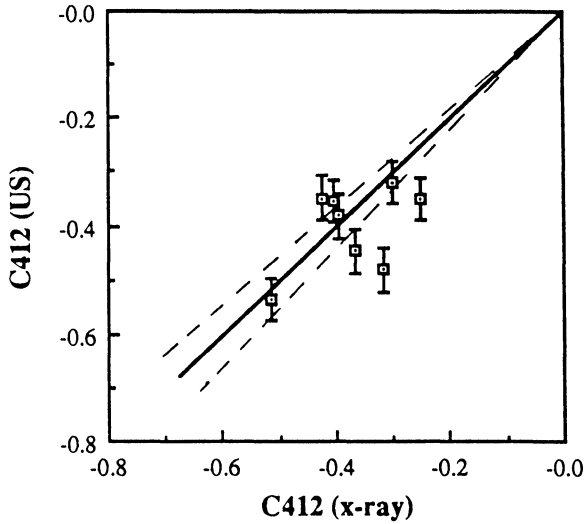


Figure 2(b). Correlation between the expansion coefficient C_4^{12} determined by ultrasonics and by X-ray diffraction for series 0.

Linear correlations between r_m and C_4^{11} determined using Eq. (3) have been confirmed previously (Spies and Schneider, 1988, Spies, 1989). The correlations between Δr and C_4^{13} for series I, IIc and IIe are shown in Figures 3 and Figures 4.

These results show that the texture coefficients C_4^{11} and C_4^{13} for the sheets tested can be related to the plastic anisotropy parameters r_m and Δr . However, the two

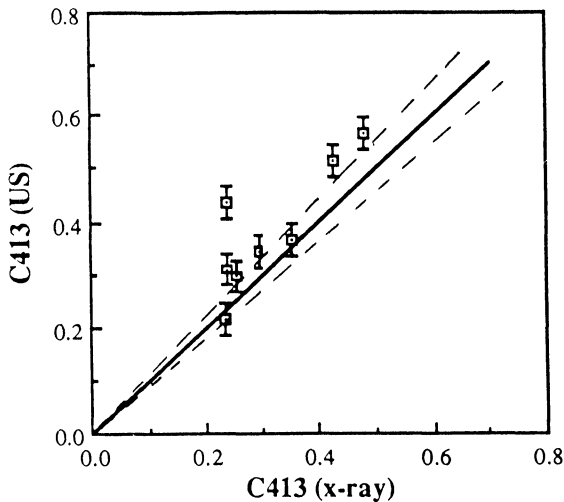


Figure 2(c). Correlation between the expansion coefficient C_4^{13} determined by ultrasonics and by X-ray diffraction for series 0.

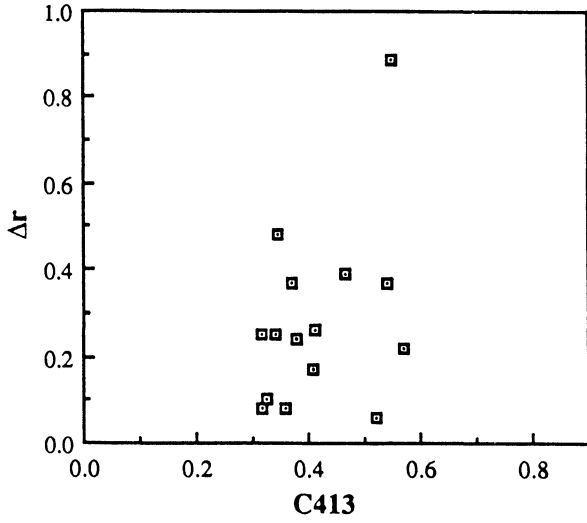


Figure 3(a). Correlation between the expansion coefficient C_4^{13} (SH-waves) and the plastic anisotropy parameter Δr for series I.

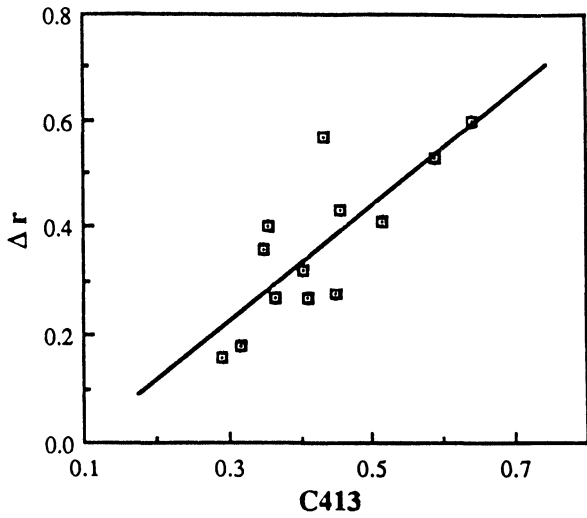


Figure 3(b). Correlation between the expansion coefficient C_4^{13} and the plastic anisotropy parameter Δr for series IIc.

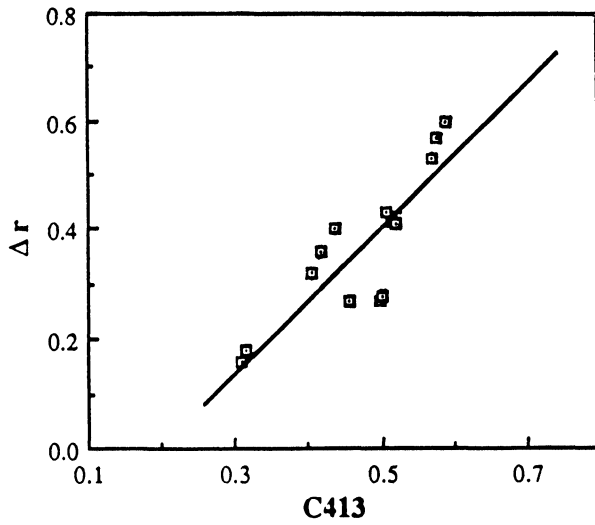


Figure 3(c). Correlation between the expansion coefficient C_4^{13} and the plastic anisotropy parameter Δr for series IIe.

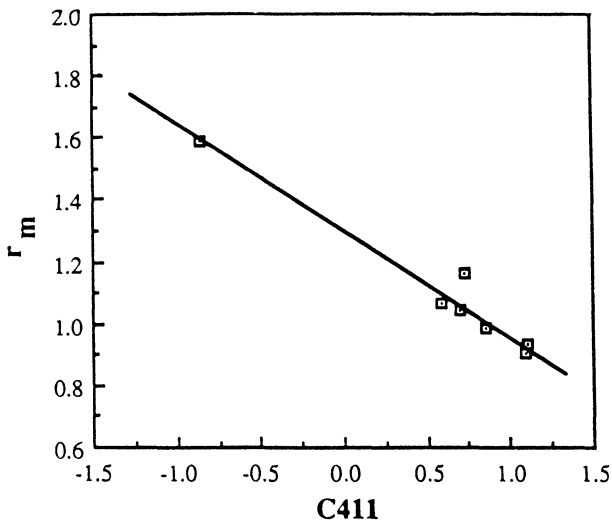


Figure 4(a). Correlation between the expansion coefficient C_4^{11} (bulk waves) and the plastic anisotropy parameter r_m for series I.

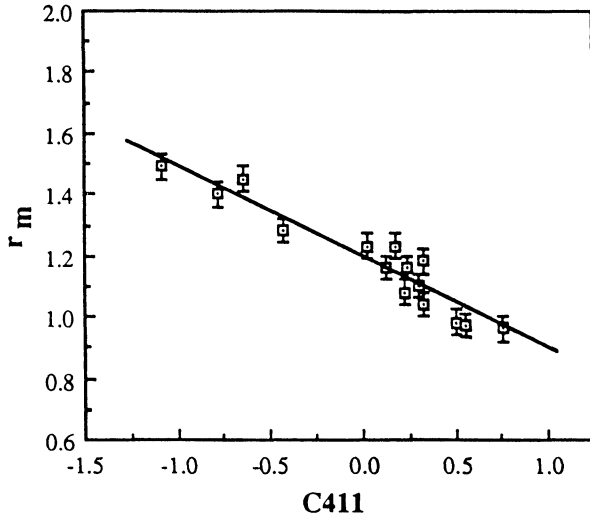


Figure 4(b). Correlation between the expansion coefficient C_4^{11} (bulk waves) and the plastic anisotropy parameter r_m for series IIc.

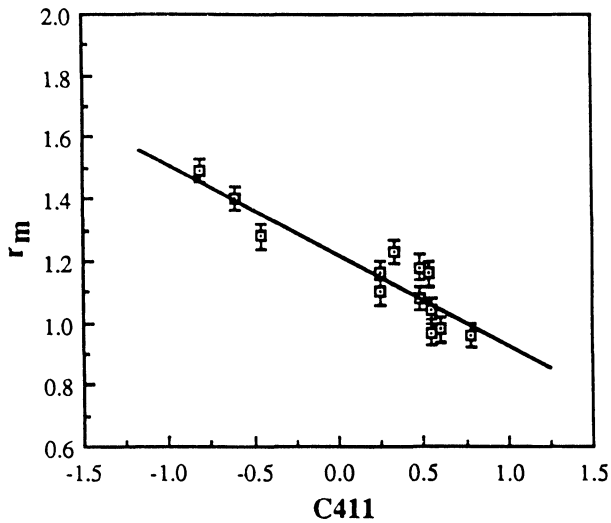


Figure 4(c). Correlation between the expansion coefficient C_4^{11} (bulk waves) and the plastic anisotropy parameter r_m for series IIe.

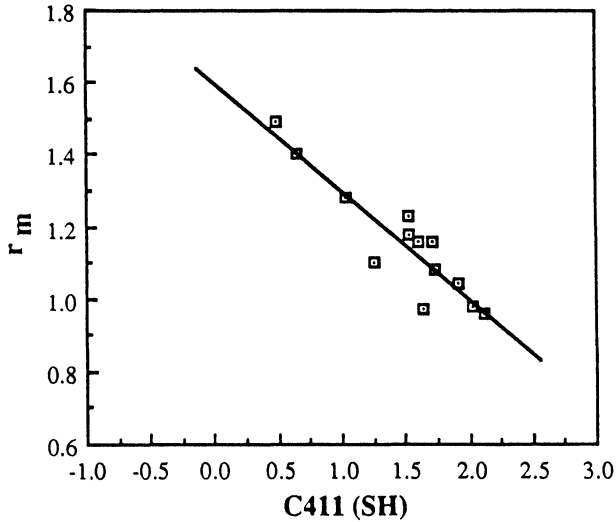


Figure 5(c). Correlation between the expansion coefficient C_4^{11} (SH-waves) and the plastic anisotropy parameter r_m for series IIe.

5. DISCUSSION

The results shown in Figures 3 to 5, which represent a part of an extensive study on hot- and cold-rolled ferritic steel sheets (Spies, 1989), confirm the expected linear correlations between r_m and C_4^{11} on the one hand and Δr and C_4^{13} on the other hand. Furthermore, the comparison of the sheets cut from the center and the edge of the coil (series II, Figures 3 and 5) seems to indicate a slight difference in the texture at these two locations. As a considerable variation in the texture and thus in the plastic behaviour over the width of the coil is extremely disturbing, an extensive study on a large number of sheets concerning this issue should provide more results to ensure reliable statistics.

The comparison of the C_4^{11} (SH)-values with those determined with shear and longitudinal waves (Spies 1989) shows that these values differ considerably. These differences are due to the applied method of generating SH-waves, which leads to a constant shift in the measured time-of-flight, and thus to a shift in the C_4^{11} (SH)-values. This effect can be eliminated by using two receiver-EMATs and measuring the time-of-flight between the respective echoes. Nevertheless, the regression lines shown in Figs. 5 are unambiguous.

The SH_0 -measurements provide good correlations between C_4^{11}/r_m and $C_4^{13}/\Delta r$. It has to be mentioned that series I (Fig. 3a) shows only poor correlation between C_4^{13} and Δr . Investigations are under way to explain these results.

Drawing a final conclusion it can be said that ultrasonics provide an efficient nondestructive method for the evaluation of the deep drawing behaviour of rolled sheets. The most important problem to be solved in order to allow an on-line application of this method is the adaption of the experimental devices to high coil velocities and to the requirement of performing non-contact measurements.

Acknowledgement

The authors like to thank Hoesch Stahl AG, Dortmund, FRG, and Thyssen Stahl AG, Duisburg, FRG, for providing the sheets examined in this work. They also like to thank Professor H. Ruppertsberg and his team, Universität des Saarlandes, Saarbrücken, FRG, for conducting the X-ray diffraction measurements.

References

- Auld, B. A. *Acoustic Fields and Waves in Solids*. Vol. 1, New York, Wiley, 1973.
- Bunge, H. J. (1965). Zur Darstellung allgemeiner Texturen. *Z. Metallkunde* **56**, 872–874.
- Bunge, H. J. (1968). Über die elastischen Konstanten kubischer Materialien mit beliebiger Textur. *Kristall & Technik* **3**, 431–438.
- Bunge, H. J. (1970). Some Applications of the Taylor Theory of Polycrystal Plasticity. *Kristall & Technik* **5**, 145–175.
- Bunge, H. J. (1982). *Texture Analysis in Materials Science*. London: Butterworth Publ. London, 1982.
- Bunge, H. J. (1982). Mean Values of Physical Properties. In *Quantitative Texture Analysis*. H. J. Bunge and C. Esling (eds.) DGM Oberursel, 383–405.
- Esling, C., Bechler-Ferry, E. and Bunge, H. J. (1982). Three-Dimensional Texture Analysis after Bunge and Roe: Correspondence Between the Respective Mathematical Techniques. *Textures and Microstructures* **5**, 95–125.
- Lankford, W. T., Snyder, S. C. and Bauscher, J. A. (1950). *Trans. ASM* **42**, 1197.
- Papadakis, E. P. Ultrasonic Phase Velocity by the Pulse-Echo-Overlap Method Incorporating Diffraction Phase Correction. *J. Acoust. Soc. Am.* **42**.
- Roe, R.-J. (1965). Description of Crystallite Orientation in Polycrystalline Materials. III. General Solution to the Pole Figure Inversion. *J. Appl. Phys.* **36**, 2024–2031.
- Sayers, C. M. and Proudfoot, G. G. (1986). Angular Dependence of the Ultrasonic SH-Wave Velocity in Rolled Metal Sheets; *J. Mech. Phys. Solids* **34**, 579.
- Spies, M. and Schneider, E. Nondestructive Analysis of the Deep-Drawing Behaviour of Rolled Sheets with Ultrasonic Techniques. Proc. of the 3rd Int. Symp. on Nondestructive Characterization of Materials, Saarbrücken, FRG, 3–6 Oct. 1988, to be published.
- Spies, M. (1989). Nondestructive Determination of Materials Textures by Ultrasonic Techniques. M.S. Thesis, University of Houston, Texas, USA; Diploma Thesis, Universität des Saarlandes, Saarbrücken, FRG.
- Stickels, C. A. and Mould, P. R. (1970). The Use of Young's Modulus for Predicting the Plastic Strain Ratio of Low-Carbon Steel Sheets. *Met. Trans.* **1**, 1303–1311.
- Thompson, R. B. Smith, J. F. and Lee, S. S. (1985). Inference of Stress and Texture from the Angular Dependence of Ultrasonic Plate Mode Velocities. In *NDE of Microstructure for Process Control*, Wadley, H. N. G. (Ed.) Metals Park, OH: *Am. Soc. of Metals* 73–79.
- Vlad, C. M. (1972). Verfahren zur Ermittlung der Anisotropie-Kennzahlen für die Beurteilung des Tiefziehverhaltens kohlenstoffarmer Feibleche. *Materialprüfung* **14**, 179–182.